New Insight into Enhanced Superconductivity in Metals near the Metal-Insulator Transition

M. S. Osofsky, R. J. Soulen, Jr., J. H. Claassen, G. Trotter, H. Kim, and J. S. Horwitz
Naval Research Laboratory, Washington, D.C. 20375
(Received 26 March 2001; published 17 October 2001)

We have studied the transport properties of disordered WSi films near the metal/insulator transition (MIT) and we have also reviewed the data for several other disordered materials near their MIT. In all cases, we found the presence of enhanced superconductivity. We constructed a superconductivity "phase diagram" (i.e., T_c versus σ) for each system, which reveals a striking correlation: In all cases, T_c values are significantly enhanced only for samples whose conductivities lie within a narrow range on the metallic side of, and moderately near, the MIT. We present a heuristic model to explain this phenomenon.

DOI: 10.1103/PhysRevLett.87.197004 PACS numbers: 74.20.–z, 74.25.Dw, 74.62.Dh

A long-standing puzzle in superconductivity is the fact that many low-temperature superconductors have dramatically enhanced superconductive transition temperatures, T_c, when they are rendered into a disordered or granular state. Examples abound: W (and W alloys) [1,2], Be (and Be alloys) [3], Ga alloys [3], Zr (and Zr alloys) [4], Al (and Al alloys) [3,5–7], Mo (and Mo alloys) [8], Re [1], V alloys [9], and Bi/Kr composites [10]. Even more striking is the fact that several other systems whose constituents usually have no, or unmeasurably low, T_c's, such as Pd [11] (and Pd alloys) [12], GeAu [13], GeAg [11,14], GeCu [11], $Si_{1-x}Au_x$ [15], and even granular Pt (with T_c around 1 mK) [16], have been shown to have measurable, and sometimes, even reasonably high T_c's.

Since the T_c enhancement is particularly strong for W alloys ($T_c = 0.015$ K for bulk W, whereas it is as high as 5 K for disordered films), we chose this system as the paradigm for the renewed study reported here. Thus, several Si-doped (0% to 30%) W films (typically 3000 Å thick) were deposited on (001) Al_2O_3 single crystal substrates by pulsed laser deposition. This range of Si doping was sufficient to cause the samples to pass from the fully conducting regime to the insulating side of the metal/insulator transition (MIT). The electrical conductivity σ was measured versus the temperature T using standard techniques, while T_c was determined both by conductivity and magnetic susceptibility. Finally, the single-particle density of states, N, was determined from point-contact tunneling using a Cu point.

In the lowest right-hand panel of Fig. 1, we plot $T_c/T_{c\ \mathrm{max}}$ for the WSi samples in this study versus the quantity r, which is proportional to σ. For comparison, we also include panels for the WSi samples in Ref. [2], as well as for four other disordered superconductors (WGe [2], MoGe [8], MoSi [8], and SiAu [15]) for which there was enough published information to construct the curve.

In seeking an explanation of the enhancement depicted in Fig. 1 for such disparate systems, it is very hard to understand how any of the conventional mechanisms (strain [7], suppression of magnetic fluctuations (in Pd) due to disorder [17], low energy or "soft" phonons [18,19], Ginzburg surface superconductivity [3], or the formation of new phases [1,17,19]) could produce curves with (i) such a sharply peaked dependence on the conductivity, (ii) with nearly the same shape, and (iii) with a maximum at a common value of r ($r \sim 12$). The dependence on σ invites a theoretical treatment based on disorder near the MIT. Indeed, several theories [20,21] have been proposed which can account for T_c as the MIT is approached ($0 < r < 12$ in the figure), but few can account for the rest of the curve ($r > 12$). We offer an explanation which is based on the fact that, as the MIT is approached, the electron screening length is enlarged by disorder. This increases

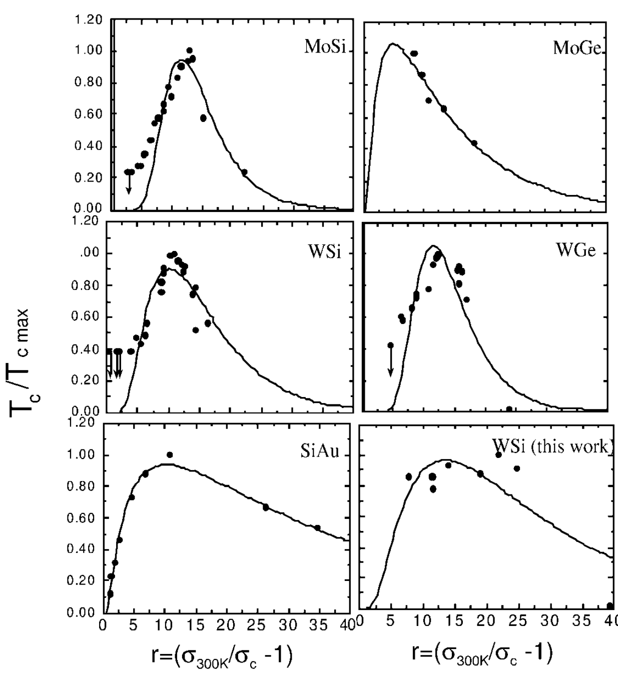

FIG. 1. Superconductivity "phase diagrams" $T_c(r)$ for six disordered metals. Data for T_c was plotted vs r for this work and for various disordered systems reported in the literature. Note that the metal/insulator transition occurs at $r = 0$. The arrows indicate that T_c is below the lowest attainable temperature of the measurement. The solid curves represent three-parameter fits of Eq. (6).

the attractive electron-phonon part of the BCS interaction V, which enhances T_c (see below). Indeed, such an enhancement mechanism has already been suggested in less explicit form for high T_c superconductivity by Bouvier and Bok [22].

The MIT is a quantum critical point. The natural coordinate near the MIT is $1/\xi \sim [(\sigma - \sigma_c)/\sigma_c]$ where, following the arguments of Osofsky *et al.* [23], we choose the room temperature value $\sigma_{300\ \mathrm{K}}$ for the conductivity σ. Thus, we write

$$1/\xi = \left(\frac{\alpha}{a}\right)\left(\frac{\sigma_{300\ \mathrm{K}} - \sigma_c}{\sigma_c}\right) = \left(\frac{\alpha}{a}\right)\left(\frac{\sigma_{300\ \mathrm{K}}}{\sigma_c} - 1\right) = \left(\frac{\alpha}{a}\right)r, \tag{1}$$

where a is the lattice parameter which defines ξ in terms of atomic dimensions, and α is a constant to be determined by experiment. Furthermore, σ_c may be determined by an experimental technique to be described below, *so that r and $(1/\xi)$ are completely defined by experimentally measured quantities.*

A scaling theory describes physical properties in terms ξ. There are several scaling theories [24–26] for behavior near the MIT, each of which make the following predictions for the metallic side when ξ is small:

$$\sigma(T) = \sigma(0)[1 + (k_B T/\Delta)^{1/2}] = \sigma_a\left(\frac{a}{\xi}\right)^{\beta}[1 + (k_B T/\Delta)^{1/2}], \tag{2}$$

$$N(V) = N(0)[1 + (eV/\Delta)^{1/2}] = N_a(a/\xi)^{\delta}[1 + (eV/\Delta)^{1/2}], \tag{3}$$

$$\Delta = \Delta_a\left(\frac{a}{\xi}\right)^{\beta\eta} \sim \sigma(0)^{\eta}, \tag{4}$$

where V is the voltage, Δ is the energy scale associated with the correlation length ξ (N.B., Δ is not the superconductive energy gap), and σ_a, N_a, and Δ_a are constants. The theories differ in the approximations used to solve the scaling equations and thus differ in the predictions for the values of the critical exponents, β, δ, and η, and in their interrelationships. Two other theories [27,28] are devoted to the "critical region" and thus are inappropriate for the experiments to be reported here.

The transport properties of the WSi films in this study exhibited all of the characteristics predicted by Eqs. (2)–(4). First, the low temperature conductivity is well described by Eq. (2) as can be seen in inset (a) of Fig. 2. The second characteristic is the development of a square-root cusp in the density of states at the Fermi energy. Figure 2, inset (b), shows the conductance versus voltage results for point-contact tunneling measurements on several WSi samples in this study where the solid lines in the figure are fits using Eq. (3). Figure 2 also demonstrates how σ_c was determined. We plotted $\sigma(T)$ in order to find the intercept at $T = 0$, thus defining $\sigma(0)$. We subsequently plotted $\sigma(0)$ versus $\sigma_{300\ \mathrm{K}}$ and the intercept defines the value σ_c at which the MIT occurs [i.e., where $\sigma(0)$ is zero]. The critical conductivity, σ_c, and thus the MIT, depends on the particular system: For the two WSi systems shown in Fig. 1, it differs by a factor of 10: $\sim$50 $(\Omega\ \mathrm{cm})^{-1}$ (this study) and 500 $(\Omega\ \mathrm{cm})^{-1}$ (Ref. [2]). Data for $\Delta[\sigma(0)]$ for this work as well as for the results of three tunneling studies of other systems [5,29,30] were fitted by Eq. (4), and the average for the four systems is $\eta = 2.2 \pm 0.1$.

To develop an expression for T_c, we first note that the net electron-electron interaction, $V(q, \omega)$, representing the sum of the positive, screened-Coulomb interaction and the attractive, phonon-mediated interaction, may be approximated many different ways. We choose the "jellium" model since the screening for both terms is given

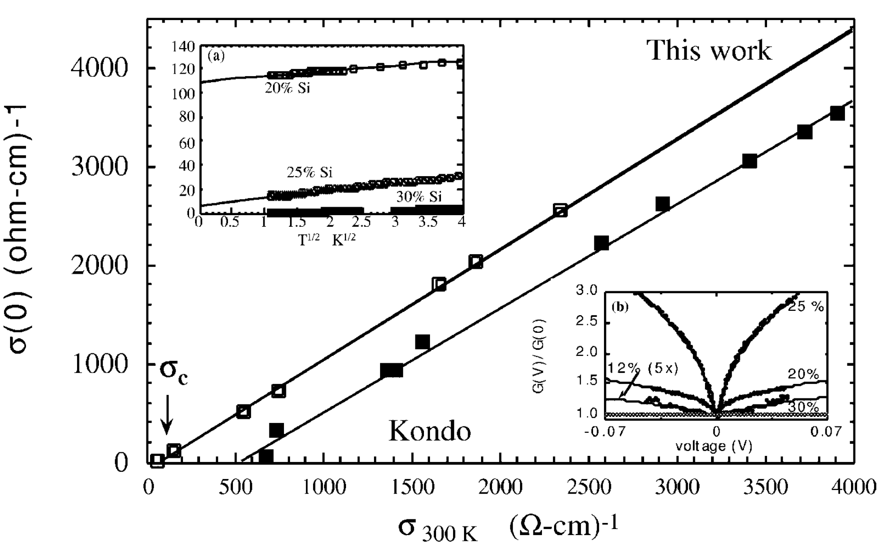

FIG. 2. Three manifestations of scaling theory for the WSi system (this work and Ref. [2]). Graph: Definition of σ_c as the intercept of $\sigma(0)$ vs $\sigma_{300\ \mathrm{K}}$. Inset (a): Conductivity vs $T^{1/2}$ for two of the WSi samples near the MIT (20% and 25% Si) (this work). The solid lines are fits of Eq. (2) to the data. Inset (b): Point contact tunneling conductance at 1.4 K for three WSi samples (this work). The solid lines are fits of Eq. (3) to the data.

explicitly [31]:

$$V(q,\omega) = \left(\frac{4\pi e^2}{q^2\varepsilon(q,\omega)}\right) = \left(\frac{4\pi e^2}{k^2+q^2}\right)\left[1+\frac{\omega_q^2}{\omega^2-\omega_q^2}\right] = \left(\frac{4\pi e^2}{k^2+q^2}\right)\left[\frac{\omega^2}{\omega^2-\omega_q^2}\right] = \left(\frac{k_s^2}{k^2+q^2}\right)(-V^*), \quad (5)$$

where $\varepsilon(q,\omega)$ is the dielectric function. We have used the definition, $k_s^2 = 4\pi e^2 N$, where k_s is the Thomas-Fermi inverse screening length. Now, far from the MIT, the screening is characteristic of a metal, in which case k_s would replace k in the dielectric function and thus in Eq. (5). However, nearer to the MIT, the scaling expression for the dielectric function implies that k is a function of ξ, which we represent as $k = (1/\xi)(a/\xi)^m$ in Eq. (5). Furthermore, following de Gennes (Ref. [31]), we choose to cut off q at $q_D \sim (3/a)$. Finally, from Eq. (3), $N = N_a(a/\xi)^\delta$. Putting all these factors together, and using the BCS result, $T_c \sim \exp(-1/NV)$, we have the following expression for T_c moderately near the MIT:

$$\begin{aligned} T_c/T_{c\ \max} &= \exp\left[\frac{-1}{N_aV^*\alpha^{\delta-2m-2}(k_s^2a^2)}\left(\frac{r^{2m+2}+(\frac{3}{\alpha^{m+1}})^2}{(r)^\delta} - \frac{(r_{\max})^{2m+2}+(\frac{3}{\alpha^{m+1}})^2}{(r_{\max})^\delta}\right)\right] \\ &= \exp\left[-A\left(\frac{r^{2m+2}+b^2}{r^\delta} - \frac{(r_{\max})^{2m+2}+b^2}{(r_{\max})^\delta}\right)\right], \end{aligned} \quad (6)$$

where

$$r_{\max} = \left[\frac{\delta(\frac{3}{\alpha^{m+1}})^2}{2m+2-\delta}\right]^{1/(2m+2)}.$$

The function given in Eq. (6) peaks at $r = r_{\max}$, and its breadth is governed by A.

In order to fit each data set shown in Fig. 1, one of the four fitting parameters had to be specified in Eq. (6), since a four-parameter fit (A, δ, m, and α) was not unique. Accordingly, we set $\delta = 1$ on the strength of the experiment of Hertel *et al.* and on the basis of fits to $(dH_{c2}/dT)_{T_c}$ given below. The results of the three-parameter fits are given in Table I. The first parameter, m, is unambiguously zero, where the value greatly simplifies the expressions in Eq. (6). It also means that $k = 1/\xi$, which identifies ξ as the screening length.

The second parameter, b, and the derived quantity α are rather constant. Indeed, the average for all six samples is $\alpha = 0.32 \pm 0.16$. This explains at once why all the curves are peaked at a common value of r. Furthermore, this value for α leads naturally to the following confirmation. Inspection of the T_c curves in Fig. 1 shows that the transition from conventional screening to the scaling region occurs at $r \sim 20$, from which we calculate $\xi = a/\alpha r \sim 0.16a \sim 0.78$ Å, which is rather close to the value of the Thomas-Fermi screening length ($1/k_s \sim 0.6$ Å). This is just what we proposed at the outset of this discussion. Using this calibration, we see that enhanced superconductivity due to scaling begins at that transition defined by $\xi \sim 0.78$ Å; it then peaks at $r = 10$, where $\xi \sim 1.6$ Å, and it disappears when $r = 5$, where $\xi \sim 3.1$ Å. We note that this range, 3 Å $< \xi <$ 1 Å, corresponds to $5 < r < 20$. Assuming that $(k_Fl) \sim 1$ at the MIT, and that this quantity is proportional to r, we have $(k_Fl) = r + 1$. Thus, $6 < (k_Fl) < 21$ over the same range. In this region, then, it is safe to use the BCS formulation of superconductivity and scaling theory as formulated above.

The final parameter is A, which may be inverted to define N_aV^* as $N_aV^* = 1/[A\alpha^{1-\eta}(k_sa)^2]$. Clearly, of the three fitting parameters, A incorporates the microscopic, sample-dependent properties. Indeed, evaluating the constants in the definition gives $N_aV^* \sim 1/77.5A$. This equation leads to very reasonable values for N_aV^*: That is, as $0.03 < A < 0.15$, we find that $0.4 < N_aV^* < 0.1$.

We may now understand the T_c curves shown in Fig. 1. Far from the MIT, in the high conductivity limit, the screening length is given by the normal Thomas-Fermi value, $1/\xi = k_s$. The product NV is that for the material in the clean limit, where T_c attains the clean-limit value, which just happens to be very small for all the materials shown in Fig. 1. As the conductivity decreases, $1/\xi$ decreases, there is reduced screening, and T_c increases since V increases. Still closer to the MIT, V is still larger but the product NV is suppressed by a disappearing N, and thus T_c plummets.

TABLE I. Fitted parameters [Eq. (6)] for six disordered systems.

Material	δ	m	A	b	$\alpha = 3/b$
WGe	1.000[a]	-0.005 ± 0.006	0.16 ± 0.04	11.6 ± 0.5	0.259
WSi	1.000[a]	-0.01 ± 0.01	0.16 ± 0.06	10.2 ± 0.8	0.294
MoSi	1.000[a]	-0.02 ± 0.009	0.15 ± 0.04	11.4 ± 0.6	0.263
MoGe	1.000[a]	0.14 ± 0.43	0.11 ± 0.05	4.3 ± 2.5	0.70
SiAu	1.000[a]	-0.04 ± 0.02	0.032 ± 0.003	9.9 ± 0.3	0.303
WSi (this work)	1.000[a]	-0.009 ± 0.017	0.053 ± 0.003	13.5 ± 1.5	0.222

[a] δ set equal to 1 in the fit.

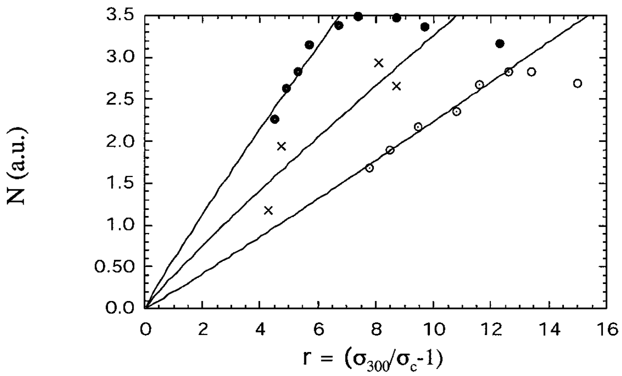

FIG. 3. Density of states, N, versus r for MoGe (solid circles), SiAu (crosses), and MoSi (open circles). In all three cases, N varies as $(1/\xi)^{\delta}$ for low values of $(1/\xi)$, and then becomes constant (two cases). The average of the three determinations is $\delta = 1.03 \pm 0.09$.

Are there further ramifications for superconductivity near the MIT? In the case of a type II superconductor, the slope of the upper critical magnetic field, H_{c2}, at T_c is proportional to $\rho_0\gamma$, where γ is the coefficient in the normal state specific heat, which in turn in proportional to N. Thus, we predict that

$$\left(\frac{dH_{c2}}{dT}\right)_{T_c} = -\left(\frac{8e^2}{\pi^2\hbar}\right)\rho_0 N \sim \rho_0\left(\frac{a}{\xi}\right)^{\delta} \sim \rho_0 r^{\delta}. \quad (7)$$

This slope was measured for the same MoGe, MoSi, and SiAu samples whose T_c values appear in Fig. 1, and furthermore γ vs Ge or Si content was calculated and reported. Using the same scheme to convert Si(Ge) content into $\sigma_{300\,\mathrm{K}}$ and σ_c as we used to construct Fig. 1, we constructed Fig. 3. It is clear from Fig. 3 that N is proportional to $(1/\xi)^{\delta}$, confirming the veracity of Eq. (3). Indeed, the average value of these three determinations is $\delta = 1.03 \pm 0.09$. Study of dH_{c2}/dT is particularly important, for it depends only on N, whereas T_c depends on the product, NV.

In conclusion, we have observed that, whenever disordered systems exhibit scaling effects in their normal-state properties, there is a concomitant enhancement in T_c. Furthermore, we have proposed that a natural phase diagram for superconductivity in this regime is $T_c(r)$ as shown in Fig. 1. We used the predictions of a BCS model, modified to account for reduced screening near the MIT, to successfully fit the $T_c(r)$ curves for six disordered systems. This model also successfully accounts for the dependence of $(dH_{c2}/dT)_{T_c}$ on r (three systems). Furthermore, all of the fitting parameters are very reasonable. Finally, the fitted values for the critical exponents obtained in this Letter ($\beta = \delta = 1$ and $\eta = 2$) are in excellent agreement with other experimental work (e.g., Hertel *et al.*). The principles established in this Letter also have many ramifications for T_c enhancement and pseudogap effects in high T_c superconductivity that will be treated elsewhere [32]. We have presented this simple, heuristic model in order to encourage a more fundamental treatment of scaling effects in low and high T_c superconductivity in the region of the MIT.

The authors wish to acknowledge useful discussions with J. Bok, J. Bouvier, S. Wolf, J. Byers, C. Kendziora, B. Nadgorny, and T. Vanderah. We also thank Y. Lyanda-Geller for many critical comments.

[1] W. L. Bond *et al.,* Phys. Rev. Lett. **15**, 260 (1965).
[2] S. Kondo, J. Mater. Res. **7**, 853 (1992).
[3] C. C. Tsuei and W. L. Johnson, Phys. Rev. B **9**, 4742 (1974).
[4] F. P. Missell and J. E. Keem, Phys. Rev. B **29**, 5207 (1984).
[5] R. C. Dynes and J. P. Garno, Phys. Rev. Lett. **46**, 137 (1981).
[6] T. A. Miller *et al.,* Phys. Rev. Lett. **61**, 2717 (1988).
[7] M. A. Noak *et al.,* Physica (Amsterdam) **135B**, 295 (1985).
[8] S. Kubo, J. Appl. Phys. **63**, 2033 (1988).
[9] H. R. Khan, Physica (Amsterdam) **135B**, 308 (1985).
[10] B. Weitzek, A. Schreyer, and H. Micklitz, Europhys. Lett. **12**, 123 (1990).
[11] B. Stritzker, Phys. Rev. Lett. **42**, 1769 (1979).
[12] H. L. Luo *et al.,* Z. Phys. B **49**, 319 (1983), and references therein.
[13] B. Stritzker and H. Wuhl, Z. Phys. **243**, 361 (1971).
[14] M. J. Burns, J. R. Lince, R. S. Williams, and P. M. Chaikin, Solid State Commun. **51**, 865 (1984).
[15] N. Nishida *et al.,* Solid State Commun. **44**, 305 (1982); M. Yamaguchi *et al.,* Physica (Amsterdam) **117B&118B**, 694 (1983); T. Furubayashi *et al.,* Solid State Commun. **55**, 513 (1985).
[16] R. Konig *et al.,* Phys. Rev. Lett. **82**, 4528 (1999).
[17] S. K. Bose, J. Kudrnovsky, I. I. Mazin, and O. K. Andersen, Phys. Rev. B **41**, 7988 (1990).
[18] J. W. Garland, K. H. Bennemann, and F. M. Mueller, Phys. Rev. Lett. **21**, 1315 (1968).
[19] Y. P. Krasny, N. P. Kovalenko, and V. A. Tesis, J. Non-Cryst. Solids **205–207**, 669 (1996).
[20] T. R. Kirkpatrick and D. Belitz, Phys. Rev. Lett. **68**, 3232 (1992), and references therein.
[21] A. M. Finkel'shtein, Physica (Amsterdam) **197B**, 636 (1994).
[22] J. Bouvier and J. Bok, Physica (Amsterdam) **249C**, 117 (1995).
[23] M. Osofsky *et al.,* Phys. Rev. B **31**, 4715 (1985); M. Osofsky *et al.,* Phys. Rev. B **32**, 2101 (1985).
[24] W. L. McMillan, Phys. Rev. B **24**, 2739 (1981).
[25] Gary S. Grest and Patrick A. Lee, Phys. Rev. Lett. **50**, 693 (1983).
[26] Yuval Gefen and Yoseph Imry, Phys. Rev. B **28**, 3569 (1983).
[27] C. Castellani, C. Di Castro, P. A. Lee, and M. Ma, Phys. Rev. B **30**, 527 (1984).
[28] A. M. Finkel'shtein, J. Exp. Theor. Phys. **59**, 212 (1984).
[29] G. Hertel *et al.,* Phys. Rev. Lett. **50**, 743 (1983).
[30] J. Lesueur, L. Dumoulin, and P. Nedellec, Phys. Rev. Lett. **55**, 2355 (1985).
[31] See, for example, P. G. de Gennes, *Superconductivity of Metals and Alloys* (Benjamin, New York, 1966).
[32] See M. S. Osofsky *et al.* (unpublished).